Mathematical Modelling and Simulation of Directly Coupled PV Water Pumping System Employing Switched Reluctance Motor

Sweta Belliwali, Aravind Chakravarti and A. B. Raju
Department of Electrical and Electronics Engineering,
B. V. B. College of Engineering and Technology,
HUBLI-580 031, KARNATAKA
Email:swetab.52@gmail.com

***Abstract*—A mathematical model and simulation of directly coupled Photovoltaic(PV) water pumping system employing Switched Reluctance Motor is considered in this paper. This system is simple and consists of a switched reluctance motor driving a centrifugal water pump powered by a PV array. This motor is cheaper, efficient and reliable than conventional AC and DC electrical machines used for this type of application. This is because of its simple construction. PV array in this system is always operated at its maximum power point (MPP) by controlling the motor input current. A simple control system has been devised to achieve maximum power point tracking of the PV array. The feasibility of this control system has been demonstrated through dynamic simulation of the system developed in MATLAB/Simulink environment. Various simulation results are presented for different insolation levels of sunlight and at different temperatures.**

I. Introduction

PV water pumping is one of the developing applications of solar energy on which considerable attention is being paid in order to increase its overall efficiency. The pumping system consists of PV array, a motor and a pump. The motors generally used are Induction Motor and DC motors.

Induction Motor is a well developed motor. It is simple, cheap and reliable, but it requires complex inverters to convert DC power to AC power with minimum harmonics. Thus, as the complexity increases its reliability in service decreases. On the other hand DC motor is the most complicated and expensive motor. It suffers from maintenance problems due to the presence of the commutator and brushes. DC motors are also associated with arcing problems which limits motor size and speed range. Hence a pumping system using SRM could be a worthy proposal because it is quite rugged, reliable, inexpensive, simple to construct and offers a relatively high torque to inertia ratio. The simple power electronic converter requirement, fault tolerance, high efficiency and capability for very high speed operations are among other advantages of SR Motor drive.

The modeling of SRM is reported in [1]–[3]. In [1], the model of SRM was developed by combining generalized electrical machine theory and finite element analysis. The model was based on inductance values calculated by finite element method for discrete time intervals. The cubic spline function had been used to provide the interpolation, thus yielding a continuous inductance profile.

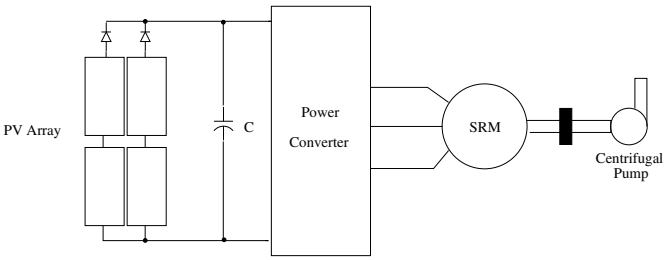

Fig. 1. Block schematic of PV pumping system

In [2], a nonlinear mathematical model of SRM based on phase winding inductance is developed. Control strategies like current chopping control and angle position control are used at low speed and high speed respectively.

In [3], a simple nonlinear model of SRM is developed based on flux linkage. Flux linkage is given as continuous mathematical expression depending on phase current and rotor position. This expression is used to get the instantaneous torque of each phase.

A PV pumping system using SRM is analyzed in [4]. The system shown uses a battery. The use of batteries does have drawbacks. Batteries can increase the cost of the overall system and this system may not work at maximum power point of the PV array. Thus the directly coupled pumping system could be a better option to increase the efficiency of this system.

II. PV Water Pumping System Under Study

In this study, a PV water pumping system using an SRM fed by power converter is considered. The schematic block diagram of the system is shown in Fig. 1. The PV array receives energy from the sunlight and generates electric power. This power is fed to the SRM through a converter. SRM drives a centrifugal pump whose output power varies as the cube of its rotor speed. With the change in the insolation level of the sunlight and at a given temperature, rotor speed varies.

978–1–4673–0315–6/11/$26.00©2011 IEEE

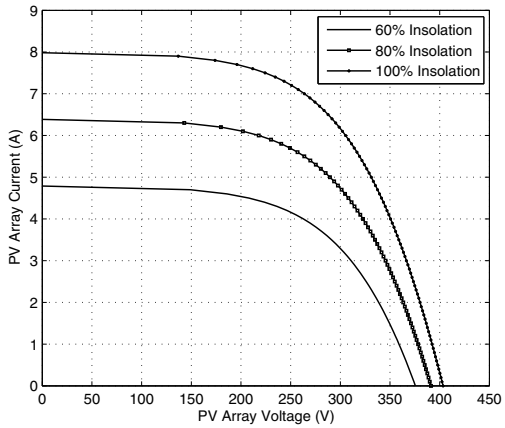

Fig. 2. Typical V-I characteristics for different insolations

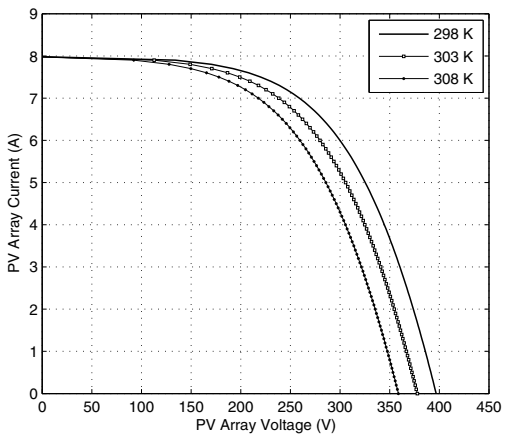

Fig. 3. Typical V-I characteristics for different temperature

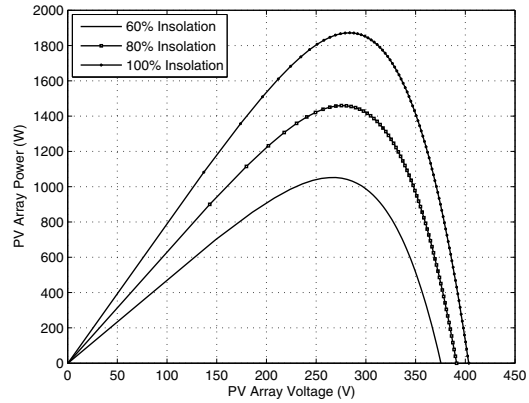

Fig. 4. Typical PV array voltage-power characteristics for different insolations

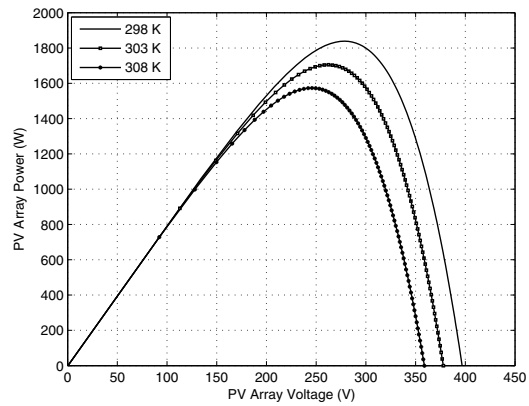

Fig. 5. Typical PV array voltage-power characteristics for different temperature

The system is operated at maximum power point of the PV array employing motor current control. The details of dynamic simulation of the system considered are presented in this paper.

A. PV Array and Output Power Characteristics

A PV array consists of several PV modules connected in series and parallel combination to provide the necessary DC voltage and current. The overall volt-ampere characteristics of the array depend on the number of cells in series and parallel strings. The PV array used in this study consists of 10 parallel strings, 748 cells in series per string, such that the overall terminal voltage v_{array} at ambient temperature is given by [5]

$$v_{array} = 54.68 \log_e \left(\frac{I_{ph} - I_{array} + 0.005}{0.005} \right) - 3.74 I_{array} \tag{1}$$

where I_{array} is the array output current in amperes and I_{ph} is a variable photo-current directly proportional to the solar insolation level (I_{ph}=8.0 A when the solar insolation is 100% or $1kW/m^2$).

Fig. 2 shows typical V-I curves for the PV array given in (1) for 60%, 80% and 100% insolation levels. It can be seen from the figure that the photo current of the array varies proportionally to the insolation. The array V-I characteristics are also affected by ambient temperature. Fig. 3 shows typical V-I curves of the PV array obtained at 100% insolation and at different temperatures. It can be seen that as the temperature increases, the array open circuit voltage decreases. Fig. 4 shows the output power versus terminal voltage of the PV array for different insolation at room temperature. It can be seen that as insolation changes the output power and MPP changes. Fig. 5 shows the power curves versus terminal voltage of the PV array for different temperatures obtained at 100% insolation. It can be seen that as temperature increases the PV array voltage and the corresponding output power decreases.

Voltage and current of the PV array at MPP can be derived by first multiplying (1) by I_{array} to obtain an expression for the output power as shown below:

$$P_{array} = 54.68 I_{array} \log_e \left(\frac{I_{ph} - I_{array} + 0.005}{0.005} \right) - 3.74 I_{array}^2$$

At maximum power,

$$\frac{dP_{array}}{dI_{array}} = 0$$

TABLE I
PV ARRAY PARAMETERS AT MAXIMUM POWER POINT

%age Insolation	V_{max} in V	I_{max} in A	P_{max} in kW
100	280.0	6.6824	1.871
75	271.97	4.9881	1.356
50	258.48	3.2972	0.852
25	231.85	1.6173	0.375

Solving these equations, the maximum power P_{max}, corresponding array voltage V_{max} and current I_{max} can be calculated and are given in Table I.

B. Switched Reluctance Motor

SRM has saliency in both stator and rotor. The stator will have concentrated type of winding and the rotor has no winding. Thus rotor is of simple construction. The principle of operation of SRM is based on the fact that a piece of magnetic material tends to align itself in the minimum reluctance position when placed in a magnetic field [6]. Fig. 6 shows cross sectional view of a 6/4 SRM. When any of the phase is excited, the rotor pole disposes itself to align with energized stator phase, thus minimizing the reluctance in the magnetic circuit. Referring to Fig. 6, if phase A is energized no torque is produced because of alignment of rotor pole with energized stator phase. However if phase C is energized, clockwise torque acts on the rotor. If phase B is energized, anticlockwise torque acts on the rotor. To produce continuous rotor motion, phases should be excited in proper sequence and at correct rotor position. The mathematical equations describing the dynamic behavior of SRM are given below [7]:

$$\theta_s = 2\pi\left(\frac{1}{N_r} - \frac{1}{N_s}\right) \quad (2)$$

$$\theta_x = \left(\frac{\pi}{N_r} - \beta_r\right) \quad (3)$$

$$\theta_y = \frac{\pi}{N_r} \quad (4)$$

$$V = \frac{d\psi_i(\theta, I_i)}{dt} + Ri \quad (5)$$

$$\psi(\theta, I_i) = L(\theta)I_i \quad (6)$$

$$T = \frac{1}{2}\frac{dL}{d\theta}I_i^2 \quad (7)$$

$$\frac{d\omega}{dt} = \frac{1}{J}(T - T_l - b\omega) \quad (8)$$

$$\frac{d\theta}{dt} = \omega \quad (9)$$

$$T_l = 0.00004166\omega^2 \quad (10)$$

where, i=1, 2, 3.

In these equations, θ_x and θ_y are the rotor position angle when it is unaligned and aligned with respect to phase-1 axis respectively as depicted in Fig. 7.

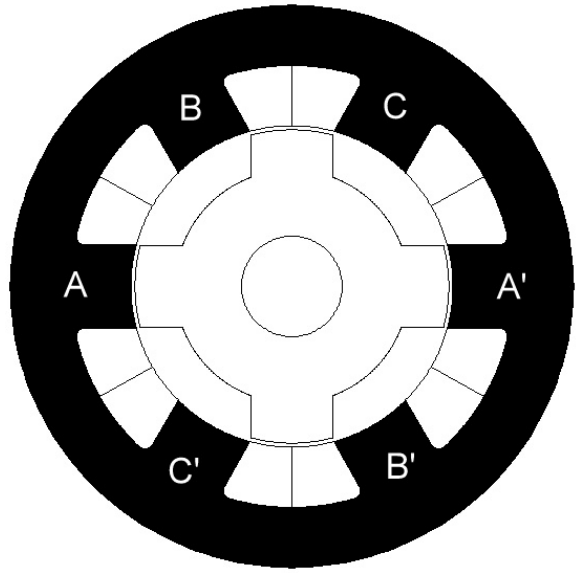

Fig. 6. 6/4 SRM

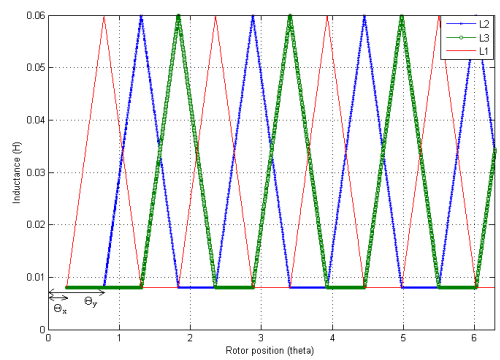

Fig. 7. Inductance profile of SRM

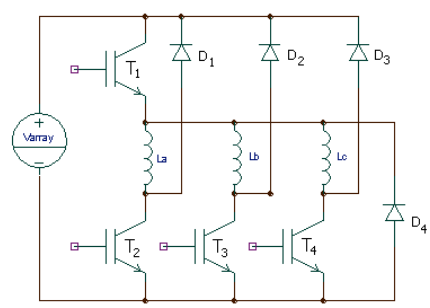

Fig. 8. Power Converter for SRM

C. Power Converter for SRM

A power converter is required to activate and commutate the SRM phases. One of such power converters is shown in Fig. 8. It is simple and economical power converter derived from conventional one. It has a single high side switching

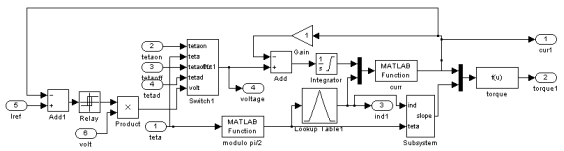

Fig. 9. Simulink model of phase-1

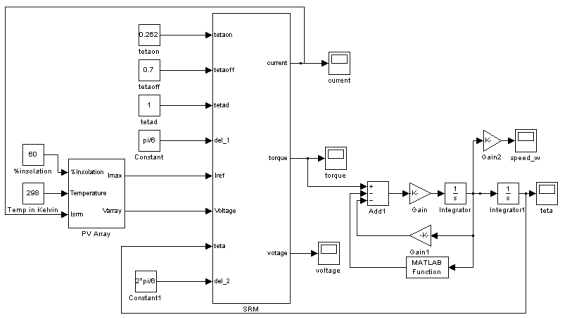

Fig. 10. Complete Simulink model of the System

device shared with all phases and a low side switching device per phase for commutation purposes. This converter is crucial for reducing the number of switching devices, diodes, floating transistor gate drives and motor connections. A disadvantage of this power converter with respect to classical converter is that phase demagnetization is affected at particularly high speed due to shorter time available for commutation.

III. Mathematical Model and Simulation Results

For the current simulation study, the SRM data has been taken from [7]. The model developed for the phase 1 is shown in Fig. 9. It contains switch, inductance profile, hysteresis, modulo pi/2, current and torque blocks.

- Switch assures the power commutation at angles θ_{on}, θ_{off} and θ_d.
- Lookup table1 gives the linear inductance profile for phase 1
- Each phase inductance has a periodicity of $\frac{2\pi}{N_r}$ degrees. Modulo pi/2 is used to transform the rotor position angle coming from the mechanical equation so that it is modulo $\frac{2\pi}{N_r}$.
- Hysteresis block is used to achieve current control, thus driving the motor at maximum power point current of PV array at given insolation level.
- Eqs. (5)–(6) are used to evaluate phase current.
- Torque block is used for the evaluation of phase torque using Eq. (7).

The model of the total system is shown in Fig. 10. It consists of the PV system, SRM, and mechanical system.

- Eq. 1 and the data in Table I are used to develop the PV system block.

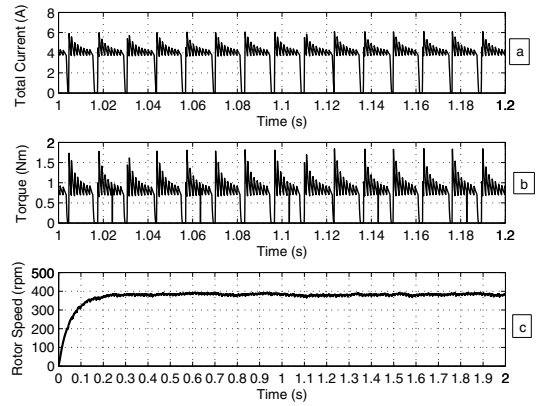

Fig. 11. Motor current, torque and speed at 60% insolation at 298 K

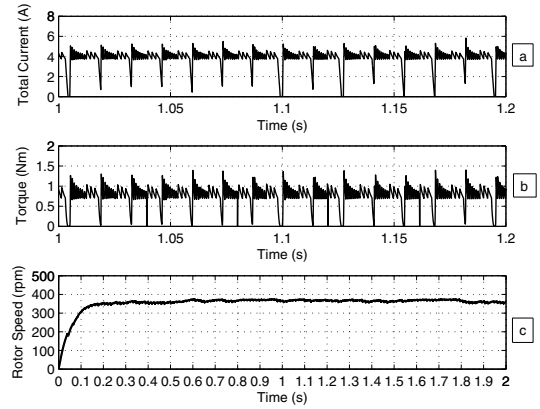

Fig. 12. Motor current, torque and speed at 60% insolation at 323 K

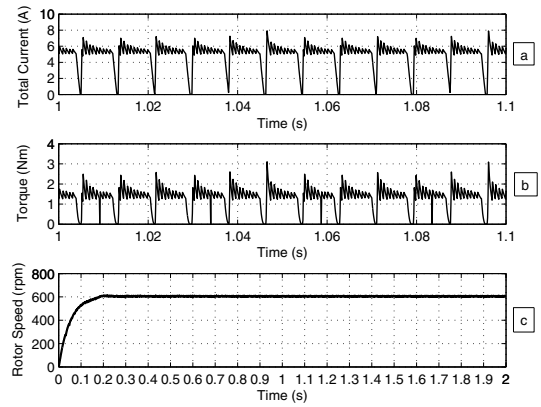

Fig. 13. Motor current, torque and speed at 80% insolation at 298 K

- Model for other two phases are developed similar to phase I using respective inductance profile. 6/4 SRM model is developed combining the model of all the three phases.
- Model for mechanical system is developed using Eqs. (8) and (9) and load torque of centrifugal pump given by Eq. (10).

The system shown in Fig. 10 has been simulated for 60% insolation and at 298K, the simulation results are presented

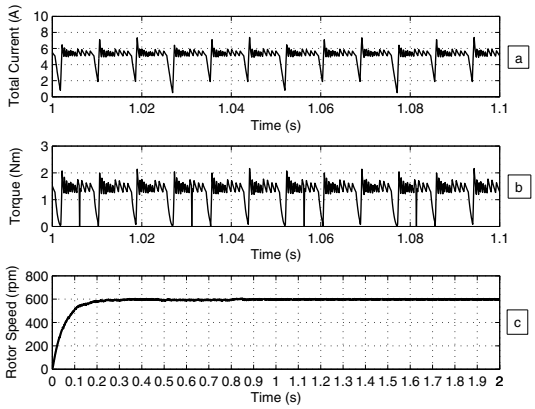

Fig. 14. Motor current, torque and speed at 80% insolation at 323 K

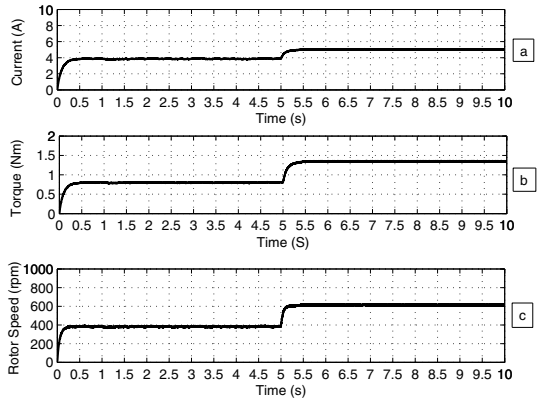

Fig. 15. Motor current, torque and speed for step change in insolation

in Fig. 11. It shows the variation of the motor current, SRM torque and speed respectively. Fig. 12 shows the variation of quantities as depicted in Fig. 11 for 60% insolation and at 323K. Similar results are shown for 80% insolation at 298K and at 323K in Figs. 13 and 14 respectively.

Figs. 15 shows the simulation results of the average PV array current, average SRM torque and speed respectively when solar insolation is varied from 60% to 80% at ambient temperature.

It can be seen from Figs. 11 to 14 that the PV array is always working at maximum power point and it can be verified from Table I. From Fig. 15 it can be seen that as the insolation level increases, the speed of the motor increases indicating that the motor output power is increasing. Whereas, as the temperature of the array increases, the speed of the motor decreases.

IV. Conclusion

A mathematical model and simulation of directly coupled PV water pumping system employing SRM is presented in this paper. PV array in this system is always operated at its maximum power point by controlling the motor input current. A simple control system has been devised to achieve maximum power point tracking of the PV array. The feasibility of this control system has been demonstrated through dynamic simulation of the system. Various simulation results are presented for different insolation levels of sunlight and at different temperatures.

Acknowledgment

The authors would like to thank Principal, B. V. B. College of Engineering and Technology, Hubli for the necessary facility provided.

References

[1] Liuchen Chung, "Modelling of Switched Reluctance Motors", *IEEE Conference CCECE'97*, pp. 866-869, 1997.

[2] Yu-Long Cui and *et. al.,*, "The Simulation Study for Switched Reluctance Motor Drives Based on Matlab 6.5", *Proceedings of Fourth International Conference on Machine Learning and Cybernetics, Guangzhou*, pp. 1076-1081, 2005.

[3] Christophe Roux and Madhat M Morcos, "On the Use of a Simplified Model for Switched Reluctance Motors", *IEEE Transactions on Energy Conversion*, Vol.17, No.3, pp. 400-405, Sept. 2002.

[4] Metwally and Anis, "Performance Analysis of PV Pumping Systems Using Switched Reluctance Motor Drives", *Energy Convers. Mgmt.*, Vol.38, No.1, pp. 1-11, 1997.

[5] S. M. Alghuwainem, "Steady-state performance of dc motors supplied from PV generators with step-up converter", *IEEE Transactions on Energy Conversion*, Vol. 7, pp.267-271, June, 1992.

[6] Fitzgerald A Kingsley, Umans S, *Electric Machinery*, New York: McGraw-Hill, 1990.

[7] F. Soares, P. J. Costa Branco, "Simulation of a 6/4 Switched Reluctance Motor Based on Matlab/Simulink Environment", *IEEE Transactions on Aerospace and Electronic Systems*, Vol.37, No.3, pp. 989-1009, 2001.